Letter

Light-induced control of magnetic phases in Kitaev quantum magnets

Adithya Sriram and Martin Claassen*

Department of Physics and Astronomy, University of Pennsylvania, Philadelphia 19104, Pennsylvania and Center for Computational Quantum Physics, Flatiron Institute, Simons Foundation, New York City 10010, New York

(Received 14 August 2021; revised 14 July 2022; accepted 20 July 2022; published 1 September 2022)

Leveraging coherent light-matter interaction in solids is a promising new direction toward control and functionalization of quantum materials to potentially realize regimes inaccessible in equilibrium, and stabilize new or useful states of matter. We show how driving the strongly spin-orbit coupled proximal Kitaev magnet α-$RuCl_3$ with circularly polarized light can give rise to a ligand-mediated magneto-electric effect that both photo induces an effective magnetic field and dramatically alters the interplay of competing exchange interactions. We propose that tailored light pulses can nudge the material toward the elusive Kitaev quantum spin liquid as well as probe competing magnetic instabilities far from equilibrium, and predict that the transient competition of magnetic exchange processes can be readily observed via pump-probe spectroscopy.

DOI: 10.1103/PhysRevResearch.4.L032036

Introduction. The search for elusive correlated and topological phases of matter, such as the Kitaev quantum spin liquid (QSL), is driven by fundamental insights and tantalizing applications that derive from their exotic properties [1]. However, their realization typically requires fine control over lattice, electronic, and magnetic interactions, a fundamental challenge in materials discovery and design [2].

An intriguing possibility involves harnessing the coherent interaction between light and matter using tailored laser pulses to drive a material out of equilibrium and modify its properties [2–4]. Seminal time-resolved experiments demonstrated coherent "dressing" of electronic bands in solids for the duration of a pump pulse [5–7], suggesting that such "Floquet engineering" could be fruitfully extended to strongly correlated systems [8–10]. Here, light can serve to selectively modify the interplay of competing interactions, and realize states of matter not readily accessible in equilibrium.

Beyond Mott-Hubbard physics recent generalizations to multiorbital systems investigated light-induced spin-orbital dynamics [11–13], or tunable exchange anisotropy, and Kitaev interactions in the presence of spin-orbit coupling [14]. However, a central challenge remains to marry Floquet engineering with the complexity of real transition metal compounds, as exemplified by recent work [15,16] on the crucial role of ligands in optically controlling magnetic states. At the same time, this added materials complexity could potentially open new pathways to selectively address electronic or magnetic properties.

Here, we predict that circularly polarized optical irradiation of a strongly spin-orbit coupled (SOC) magnet, α-$RuCl_3$—a candidate Kitaev material—grants a twofold handle to control the magnetic state. First, the chirally oscillating electric field component can induce a large ligand-mediated effective magnetic field in the [111] direction, the field direction required to induce a gap in the Kitaev model. Second, an optical pulse can selectively modify the interplay between ligand superexchange and direct exchange, thereby dramatically altering the balance between isotropic and anisotropic magnetic interactions. These effects can conspire to drive the material toward a nonequilibrium realization of the Kitaev QSL. We predict that resulting transient modifications of the magnetic dynamics can be readily observed in time-resolved probes of the excitation spectrum, and find a host of competing instabilities that can be probed out of equilibrium.

Light-matter interaction in Kitaev magnets. In Kitaev materials such as $RuCl_3$, a single hole resides in the t_{2g} manifold of the transition metal (TM) d orbitals, which splits into $j_{\text{eff}} = 1/2$ and $j_{\text{eff}} = 3/2$ states via strong SOC to form an effective spin-1/2 local moment [17–23]. Fortuitous interference of ligand-mediated superexchange processes along the $\sim 90^\circ$ Ru-Cl-Ru bond gives rise to the Kitaev interaction $K\hat{S}_i^\gamma \hat{S}_j^\gamma$, with $\gamma = x, y, z$ along the three inequivalent bonds that form a honeycomb lattice. Conversely, subdominant Heisenberg and off-diagonal anisotropic interactions arise mainly from direct TM-TM exchange and instead induce conventional zigzag magnetic order in $RuCl_3$.

The geometric dependence of exchange processes underlying each of the competing magnetic interactions, combined with strong SOC, suggests that tailored light pulses can in principle selectively enhance or suppress certain desired processes and nudge the material towards a QSL. To describe this effect, consider α-$RuCl_3$ irradiated with a broad circularly polarized light pulse, with the plane of polarization in the octahedral plane. For a single octahedron, the dynamics of holes in the Ru t_{2g} orbitals and charge-transfer (CT) excitations to

*claassen@sas.upenn.edu

Published by the American Physical Society under the terms of the Creative Commons Attribution 4.0 International license. Further distribution of this work must maintain attribution to the author(s) and the published article's title, journal citation, and DOI.

the edge-sharing ligand p orbitals are given by [20]

$$\hat{H}_0 = U\sum_{i\alpha}\hat{n}_{i\alpha\uparrow}\hat{n}_{i\alpha\downarrow} + \sum_{i\sigma\sigma',\alpha<\beta}(U' - \delta_{\sigma\sigma'}J_H)\hat{n}_{i\alpha\sigma'}\hat{n}_{i\beta\sigma} + J_H\sum_{i,\alpha\neq\beta}(\hat{c}^\dagger_{i\alpha\uparrow}\hat{c}^\dagger_{i\alpha\downarrow}\hat{c}_{i\beta\downarrow}\hat{c}_{i\beta\uparrow} - \hat{c}^\dagger_{i\alpha\uparrow}\hat{c}_{i\alpha\downarrow}\hat{c}^\dagger_{i\beta\downarrow}\hat{c}_{i\beta\uparrow}) + \frac{\lambda}{2}\sum_i \mathbf{c}_i^\dagger(\mathbf{L}\cdot\mathbf{S})\mathbf{c}_i + \Delta\sum_{i'}\hat{p}^\dagger_{i'\sigma}\hat{p}_{i'\sigma} \quad (1)$$

Here, indices i and i' sum over TM and ligand sites respectively, and U, U', J_H denote intraorbital, interorbital Coulomb interactions, and Hund's coupling for orbitals $\alpha, \beta \in \{d_{yz}, d_{xz}, d_{xy}\}$. Furthermore, Δ parametrizes the ligand CT energy with ligand fermionic operators $\hat{p}^\dagger_{i'\sigma}$, and λ denotes the atomic SOC.

Direct and ligand-mediated hopping of holes between neighboring Ru sites is constrained by the rotational symmetry of the octahedral plane [20,24]. Here, minimal coupling between light and electrons entails a Peierls substitution $\hat{c}^\dagger_i\hat{c}_j \to e^{i\frac{e}{\hbar}\mathbf{r}_{ij}\cdot\mathbf{A}(t)}\hat{c}^\dagger_i\hat{c}_j$, where $\mathbf{r}_{ij}$ are bond vectors projected onto the octahedral plane and $\mathbf{A}(t) = A[\sin(\Omega t), \cos(\Omega t)]$ is the vector potential for a circularly polarized laser with frequency Ω. We henceforth denote the field strength via the dimensionless parameter $\bar{A} \equiv a_0 e\mathcal{E}/(\hbar\Omega)$, with a_0 and $\mathcal{E}$ the TM-TM distance and peak electric field, respectively [25]. Importantly, the different hopping matrix elements acquire geometrically dependent phase factors

$$\hat{H}'_{ij}(t) = \sum_\sigma\Bigg\{\hat{\mathbf{d}}^\dagger_{i\sigma}\cdot e^{i\mathbf{r}_{ij}\cdot\mathbf{A}(t)}\cdot\begin{bmatrix} t_1 & t_2 & t_4\\ t_2 & t_1 & t_4\\ t_4 & t_4 & t_3\end{bmatrix}\cdot\hat{\mathbf{d}}_{j\sigma} + t_{pd}(e^{i\mathbf{r}_{i'i}\cdot\mathbf{A}(t)}\hat{p}^\dagger_{i'\sigma}\hat{c}_{id_{yz}\sigma} + e^{i\mathbf{r}_{ji'}\cdot\mathbf{A}(t)}\hat{c}^\dagger_{jd_{xz}\sigma}\hat{p}_{i'\sigma} + e^{i\mathbf{r}_{j'i}\cdot\mathbf{A}(t)}\hat{p}^\dagger_{j'\sigma}\hat{c}_{id_{yz}\sigma} + e^{i\mathbf{r}_{jj'}\cdot\mathbf{A}(t)}\hat{c}^\dagger_{jd_{xz}\sigma}\hat{p}_{j'\sigma}) + \text{H.c.}\Bigg\}, \quad (2)$$

with $\hat{\mathbf{d}}^\dagger_{i\sigma} = [\hat{c}^\dagger_{id_{xz}\sigma}\ \hat{c}^\dagger_{id_{yz}\sigma}\ \hat{c}^\dagger_{id_{xy}\sigma}]$ and i', j' the two ligands at the corners of edge-sharing octahedra that encase TM neighbors i, j along a Z bond.

For sufficiently broad pump pulses, the Hamiltonian becomes approximately symmetric under discrete time translations $t \to t + 2\pi/\Omega$ near the pulse maximum, with $T = 2\pi/\Omega$. In this case, Floquet theory permits a representation of the period-averaged transient dynamics in terms of eigenstates of an effective time-independent Hamiltonian and associated eigenenergies, which are defined modulo Ω due to lack of energy conservation. An equivalent frequency domain representation of Floquet theory seeks eigenstates of a Hamiltonian $\mathcal{H} = \sum_{mm'}(\hat{H}_{m-m'} + m\Omega\delta_{mm'})|m\rangle\langle m'|$ defined in a product space of the original Hilbert space and the space of periodic functions, with $\hat{H}_m = (1/T)\int_0^T dt\, e^{im\Omega t}\hat{H}(t)$ a Fourier expansion of the Hamiltonian $\hat{H}_0 + \sum_{\langle ij\rangle}\hat{H}'_{ij}(t)$ [26]. Physically, this Hamiltonian describes the "dressing" of the original Hamiltonian with absorbed/emitted photons with frequency Ω, in the semiclassical limit of a strong coherent field.

Central to this proposal, photon dressing of electronic states entails transient modifications of the magnetic interactions which discern between ligand-mediated and direct exchange processes, as well as the generation of an effective magnetic field (an inverse Faraday effect). Both can be readily derived via a strong-coupling expansion which simultaneously eliminates charge excitations and photon absorption/emission events [8–10], and remains valid on prethermal time scales as long as the local $J = 1/2$ moment persists. As ligand-mediated (t_{pd}) processes are essential to this description, the expansion must at minimum proceed to fourth order in t_{pd}. Circular polarization preserves rotations in the plane of polarization, and so symmetry dictates that the resulting photo-modulated exchange interactions remain described via modified parameters J, K, Γ, Γ', which crucially all become functions of the pump parameters $\bar{A}$, Ω [26]. Conversely, time-reversal symmetry is broken by the field; combined with broken spin rotation symmetry due to strong SOC, this additionally necessitates the emergence of an effective photoinduced magnetic field h_{ME}. This inverse Faraday effect in a Mott insulator results purely from coupling the oscillating *electric field* component of the pulse to electronic motion. Approximate C_3 rotation symmetry dictates that h_{ME} must point in the [111] direction, precisely the direction required to open a gap for the non-Abelian phase of the Kitaev model. We arrive at the following prethermal magnetic Hamiltonian where all coefficients are understood to be functions of $\bar{A}$, Ω :

$$\hat{H} = \sum_{\langle ij\rangle_{\gamma(\alpha\beta)}}\mathbf{S}_i\cdot\begin{pmatrix} J & \Gamma & \Gamma'\\ \Gamma & J & \Gamma'\\ \Gamma' & \Gamma' & J + K_\gamma\end{pmatrix}\cdot\mathbf{S}_j + h_{\text{ME}}\sum_i\hat{\mathbf{n}}_{111}\cdot\mathbf{S}_i, \quad (3)$$

with $\hat{\mathbf{S}}_i^T = [\hat{S}_i^\alpha\ \ \hat{S}_i^\beta\ \ \hat{S}_i^\gamma]$ and $\hat{\mathbf{n}}_{111}$ denotes the unit vector in [111] direction. Importantly, all coefficients are understood to be functions of $\bar{A}$, Ω, and are determined numerically using a standard fourth-order strong-coupling expansion of the electronic Floquet Hamiltonian $\mathcal{H}$ defined above [27].

Results for the transient modification of Kitaev exchange (normalized to $\sqrt{K^2 + J^2 + \Gamma^2 + (\Gamma')^2 + h_{\text{ME}}^2} = 1$) and the effective magnetic field are shown in Figs. 1(a) and 1(b). Notably, the effect of the pump is twofold. First, photon-dressing of the bonds leads to a bond-length-dependent renormalization of the hopping amplitudes, thereby discriminating between TM-ligand and TM-TM hopping. Second, photon absorption lowers virtual intermediate state energies. In combination, a tailored pulse can hence target the vicinity of t_{2g} excitations, thereby enhancing K and significantly suppressing non-Kitaev interactions [Fig. 1(c)], nudging the material towards the QSL.

Inverse Faraday effect. The microscopic origin of the photoinduced magnetic field is readily identified as ligand-mediated *third-order* virtual tunneling processes of holes around triangles spanned by TM-ligand-TM bonds in the presence of strong spin-orbit coupling. In equilibrium or without SOC, such processes are required to vanish in the absence of external magnetic fields, reflecting perfect destructive interference between clockwise and counter-clockwise hopping pathways. This situation changes dramatically in the driven system. Here, a hole can virtually absorb and emit a photon upon hopping along the noncollinear d–d and

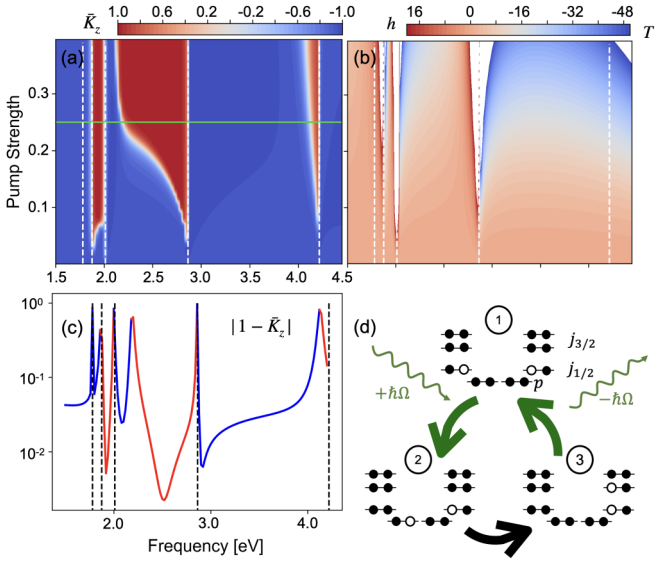


FIG. 1. Variation of Kitaev interaction (a) and effective magnetic field (shown in Tesla) (b) with pump parameters. Kitaev exchange $\bar{K}$ is normalized so that the magnetic coefficients output by the calculation of the model in Eq. (3) are set to an energy scale of one, with $(K^2 + J^2 + \Gamma^2 + \Gamma'^2 + h_{ME}^2)^{1/2} \equiv 1$. Dashed white lines mark intra-t_{2g} resonances. (c) Shows variation of $\bar{K}$ with frequency for a fixed pump frequency (green line). In a region of drive frequencies (around $\Omega = 2.5$) $\bar{K}$ approaches unity, corresponding to the Kitaev point. (d) Leading third-order time reversal symmetry breaking process responsible for the inverse Faraday effect. The chirality of the pump leads to inequivalent interference between clockwise and counter-clockwise virtual hopping of holes along TM-ligand-TM loops.

p–d- bonds of a triangle [Fig. 1(d)], thereby picking up an overall phase to avert cancellation with the directionally reversed "partner" process. This phase in turn depends on the ligand bond angle.

As the contribution to individual TM sites must follow from a sum of processes along X, Y, Z bonds, approximate C_3 rotation symmetry entails that the total induced magnetic field points in the [111] direction. Its quantitative dependence on pump strength and frequency is depicted in Fig. 1(b), including up to fourth-order hopping processes. While the magnetic field experiences a series of sign changes that coincide with intermediate-state resonances, it is instructive to approximate the photo-induced magnetic field for low-frequency pumping near the first resonance

$$h_{\mathrm{ME}}(A,\Omega) \approx \frac{A^2 \sin(\phi)\, t_{pd}^2\, (t_1 - t_3)}{36 r_{pd}\left(U - 3J_H - \frac{3}{2}\lambda - \Omega\right)}\left(\frac{1}{\Delta} - \frac{1}{\Delta + \Omega}\right). \tag{4}$$

Here, ϕ denotes the bond angle between TM-TM and TM-ligand bonds projected into the plane of polarization, and r_{pd} is the relative TM-ligand bond length compared to the direct TM-TM distance.

Spectroscopic Signatures. Armed with predictions for light-induced magnetic interactions, we now turn to consequences for the transient magnetic state. There are two prescient questions: (1) Can the coherent modification of the local exchange interactions predicted by the Floquet picture be observed in time-resolved pump probe experiments where energy absorption is an obstacle? (2) Does the prethermal steady state phase diagram include a nonequilibrium Kitaev QSL phase that can be reached with optical means?

To address the former, we employ large-scale numerical simulations of an electronic 18-orbital "Ru_4Cl_6" cluster [Fig. 2(a)] to study a nonequilibrium generalization of the dynamical $q = 0$ spin structure factor [28]

$$S(\omega, t_p) = \int dt dt' e^{i\omega(t-t')} f_{t_p}(t) f_{t_p}(t') \langle \hat{S}^z(t) \hat{S}^z(t') \rangle, \tag{5}$$

where $\hat{S}^z = (1/2)\sum_{n\alpha}(\hat{n}_{n\alpha\uparrow} - \hat{n}_{n\alpha\downarrow})$ and $f_{t_p}(t) = e^{-(t-t_p)^2/2\sigma_p}$ are Gaussian probe shape functions with width σ_p centered at the probe time t_p. The two-time spin correlation function is calculated from time evolution of the exact electronic many-body wave function [26]. This permits a direct study of the resulting photoinduced magnon spectrum for realistic pulse envelopes, to assess the competition between coherent control and heating.

Starting from the equilibrium ground state, a wide ($\sim$1 ps) Gaussian pulse with circular polarization irradiates the system, and a second Gaussian probe pulse measures the magnetic response [Fig. 2(b)]. To assess the maximal change of the magnetic excitation spectrum, we probe the dynamical spin response [Eq. (5)] at the peak of the pump pulse. Figures 2(c) and 2(d) depict the pump strength dependence for two pump frequencies $\Omega = 0.8$ eV and $\Omega = 1.2$ eV, respectively. While energy absorption from the pump would naively be expected to suppress magnetism, the observed response exhibits a *coherent* hardening of higher-energy magnetic excitations at weak pump strengths. This behavior corresponds to a prethermal enhancement of magnetic exchange interactions as predicted above. Figure 2(e) shows qualitatively analogous steady-state predictions for the Floquet spin Hamiltonian (Fig. 1) as a function of pump strength at $\Omega = 0.8$ eV, with equilibrium discrepancies of excitation energies attributable to charge fluctuations that are amiss in a purely magnetic description. Beyond a critical pump strength, the magnetic peaks are rapidly suppressed due to heating [Fig. 2(f)]. This melting of the magnetic sector at $A \approx 0.4$ ($\approx$0.2 for $\Omega = 1.2$ eV) coincides with a time-dependent suppression of magnetic moments [Fig. 2(g)], which approach their infinite-temperature expectation values beyond the critical pump strength. Finally, while the ground state in equilibrium has zero net magnetization, the inverse Faraday effect contribution can also be individually probed from time-dependent induced magnetization oscillations. Figure 2(h) depicts the peak magnetization $\max|\langle S^z(t)\rangle|$ as a function of pump strength near the pump maximum, which matches the $\sim A^2$ scaling as expected from Floquet predictions.

Floquet phase diagram. To assess whether the predicted optical control of the magnetic interactions can nudge the system towards a QSL phase, we now turn to studying the transient phase diagram via exact diagonalization of the photomodulated *magnetic* Hamiltonian for a larger 24-site cluster. Physically, this corresponds to the limit in which the equilibrium state can transform close to adiabatically to the corresponding prethermal Floquet state for slow switch-on of

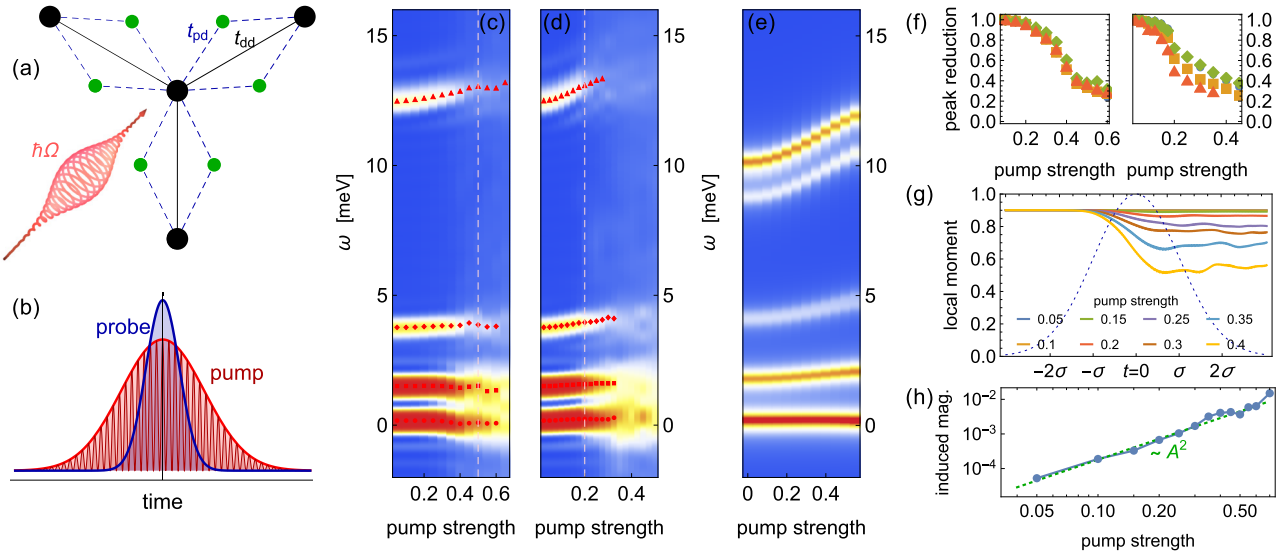


FIG. 2. (a) A ten-atom (18-orbital) TM-ligand cluster, consisting of a TM ion with three nearest neighbors with X, Y, Z bonds, is irradiated (b) with a broad circularly polarized pump pulse, with the magnetic response obtained from a probe pulse centered at the pump maximum. (c), (d) Pump-probe $\mathbf{q} = 0$ dynamical spin structure factor as a function of peak pump strength A for $\Omega = 0.8$ eV, 1.2 eV, respectively, evaluated for a 10-atom (18-orbital) cluster [inset] and probed at the peak of the Gaussian pulse. Weak fields reveal coherent modifications of the magnon spectrum, whereas the magnetic sector melts beyond a critical pump strength (dashed lines). (c) Shows analogous steady-state predictions from the photomodulated spin model, with deviations in equilibrium from the electronic model attributable to absence of charge fluctuations. (e), (f) Pump-induced suppression of the four depicted magnetic peaks [$\Omega = 0.8$ eV, 1.2 eV], corresponding to peak markers ○, □, ◇, △ in (a), (b). Melting of magnetic excitations for stronger fields coincides with time-dependent suppression of the local moment (g), which saturates for weak fields while approaching its infinite-temperature expectation value for strong pumping. (g) Transiently induced magnetization oscillations $\langle \hat{S}^z(t) \rangle$ serve as a direct probe of the inverse Faraday effect.

the drive, effectively identifying phase boundaries that remain inaccessible in equilibrium but can be reached by driving, and effectively delineates reachable out-of-equilibrium phase transitions for appropriately tailored pulses. The steady-state phase diagram is depicted in Fig. 3 as a function of pump strength and frequency, with the particular region of pump parameters shown corresponding to a region where the Kitaev interaction is predicted to be sufficiently dominant as to stabilize a QSL [Fig. 1(c)]. Phase boundaries were determined from singular features in $-\frac{\partial^2 E}{\partial \omega^2}$, and phases were identified from the value of the plaquette flux operator $W_p = 2^6 S_i^x S_j^y S_k^z S_l^x S_m^y S_n^z$ (± 1 for the QSL) [Fig. 3(a)] and spin correlation functions [Fig. 3(b)]. Notably, the pump parameters provide handles to traversing the $JK\Gamma\Gamma'$ phase diagram, suggesting that the equilibrium zigzag (ZZ) phase of $RuCl_3$ could be pushed into a number of proximal phases.

There are two striking features of the identified spin liquid phase. First, although $RuCl_3$ is proximate to a ferromagnetic-K QSL, we find here that the optimal choice of pump parameters leaves the sign of K transiently inverted. Second,

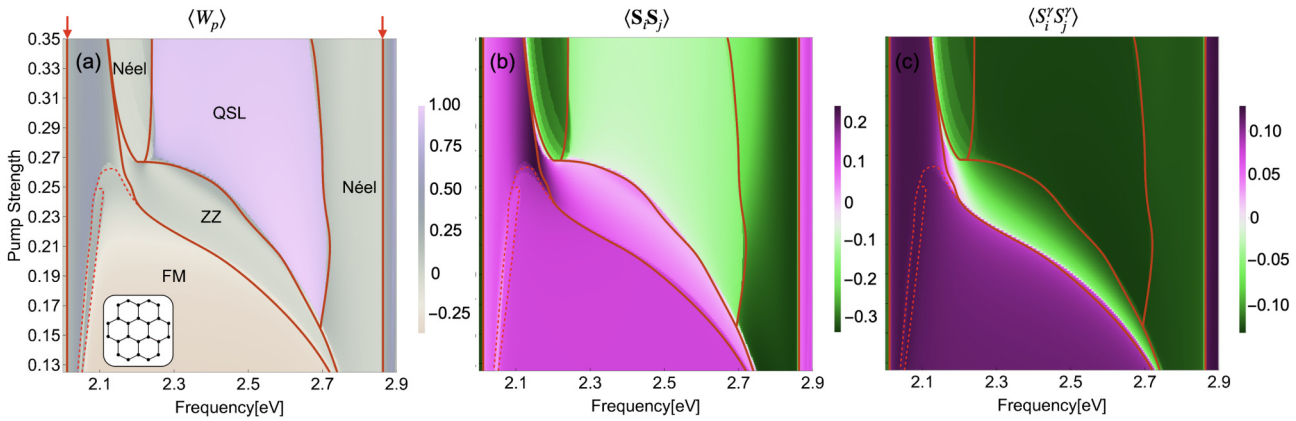


FIG. 3. Steady-state phase diagram of Floquet spin model. Color shows magnitude of $\langle W_p \rangle$ for (a), $\langle \mathbf{S}_i \mathbf{S}_j \rangle$ for (b), and $\langle S_i^\gamma S_j^\gamma \rangle$, where γ is the Kitaev direction, for (c) that led to phase identification. In the QSL phase, $\langle W_p \rangle \approx 1$, $\langle \mathbf{S}_i \cdot \mathbf{S}_j \rangle \approx \pm 0.131$. Red arrows denote resonances. Red lines marking phase boundaries are a guide for the eye. Dashed red line marks a possible phase boundary between the ferromagnetic phase and a phase that we could not conclusively identify. Inset shows the exact diagonalization cluster used.

in contrast to the equilibrium phase diagram [18,19,26,29], the identified QSL occupies a robust and wide range of the parameter space. This can be attributed precisely to the dynamical inverse Faraday effect that gaps out the QSL, consistent with recent theoretical studies on QSL stability in a magnetic field [30]. Furthermore, a small but nonzero Γ' is also purported to stabilize the QSL phase [31]. Finally, we remark on the dashed red lines shown in [3]. In the region where $2 < A < 2.1$, the spin exchange coefficents derived from the Floquet calculation take on values which place the system in a phase that is possibly ferromagnetic, incommensurate spiral or zigzag. However, there is not widespread agreement on what the resulting phase is and we were unable to readily identify it [19,29].

Discussion. We have shown that optical irradiation of α-$RuCl_3$ can grant a twofold handle to transiently alter competing magnetic interactions and induce an effective magnetic field, thereby coherently manipulating the magnetic state. Predicted spectroscopic signatures of coherent control presented above are readily accessible in time-resolved experimental probes of the magnetic excitation spectrum.

A lingering question regards possible time resolved signatures of spin liquid behavior out of equilibrium. Here, the central conclusion drawn from the steady-state phase diagram established in this work is that the equilibrium zigzag state can be "nudged" toward the QSL regime using an appropriately tailored pulse. Therefore, an intriguing consequence is the possibility for signatures of phase boundaries in the spectroscopic response. For instance, we speculate that Kerr and Faraday rotation, while generally yielding a response upon circularly polarized irradiation, may be effective at detecting changes in corresponding phase boundaries between photoinduced phases (e.g., AFM to QSL). The pump strengths presented here should be accessible experimentally [32]. We also note that understanding the pulse shape dependence of such prethermal nonequilibrium phase transitions remains an interesting open problem [33].

Furthermore, while energy absorption from the pump melts magnetic order at higher pump strengths as shown above, a general omission in Floquet engineering studies of correlated materials is the lack of energy dissipation to the lattice or other degrees of freedom. Here, an important open question concerns the role of energy absorption, dissipation, and decoherence in stabilizing or destabilizing transiently engineered nonequilibrium states.

Finally, the electronic model for $RuCl_3$ remains under considerable debate, with a minimal description utilized in this work neglecting the e_g orbitals of the TM as well as longer-ranged exchange processes beyond nearest neighbors. The former contribute to magnetic exchange [18]. However, *ab initio* studies of $RuCl_3$ that neglect t_{2g}-e_g mixing have successfully captured magnetic properties in equilibrium [20,34]; inclusion of e_g orbitals is hence not expected to significantly alter our results as long as direct resonances are avoided. For the latter, several studies remarked on the importance of third-neighbor interactions in stabilizing the equilibrium zigzag phase [20,29,35]. However, it is unclear whether the Γ' interaction or the J_3 interaction is more important in this regard [35]. Their relative importance away from equilibrium hence remains an open question for future work.

Importantly, the predicted mechanism readily generalizes to other spin-orbit coupled magnets, including the honeycomb Kitaev materials such as Na_2IrO_3 and α-Li_2IrO_3. Here, while details of the relative competition of magnetic parameters can differ dramatically, a central thread is the possibility to leverage the added materials complexity of ligand-mediated interactions to provide a knob to both affect the interplay of anisotropic exchange and induced magnetic fields in a controlled manner, to steer the magnetic state. We therefore expect that our analysis can be readily applied to a variety of frustrated magnetic systems.

Acknowledgments. We would like to thank Liang Wu and James McIver for helpful comments and discussions. We are grateful for hospitality and support from the Center for Computational Quantum Physics at the Flatiron Institute, a division of the Simons Foundation, where part of this work was performed.

[1] B. Keimer and J. E. Moore, The physics of quantum materials, Nat. Phys. **13**, 1045 (2017).

[2] D. N. Basov, R. D. Averitt, and D. Hsieh, Towards properties on demand in quantum materials, Nat. Mater. **16**, 1077 (2017).

[3] A. de la Torre, D. M. Kennes, M. Claassen, S. Gerber, J. W. McIver, and M. A. Sentef, Nonthermal pathways to ultrafast control in quantum materials, Rev. Mod. Phys. **93**, 041002 (2021).

[4] T. Oka and S. Kitamura, Floquet engineering of quantum materials, Annu. Rev. Condens. Mater. Phys. **10**, 387 (2019).

[5] Y. H. Wang, H. Steinberg, P. Jarillo-Herrero, and N. Gedik, Observation of Floquet-Bloch states on the surface of a topological insulator, Science **342**, 453 (2013).

[6] F. Mahmood, C.-K. Chan, Z. Alpichshev, D. Gardner, Y. Lee, P. A. Lee, and N. Gedik, Selective scattering between Floquet-Bloch and Volkov states in a topological insulator, Nat. Phys. **12**, 306 (2016).

[7] J. W. McIver, B. Schulte, F. U. Stein, T. Matsuyama, G. Jotzu, G. Meier, and A. Cavalleri, Light-induced anomalous hall effect in graphene, Nat. Phys. **16**, 38 (2020).

[8] M. Bukov, M. Kolodrubetz, and A. Polkovnikov, Schrieffer-Wolff Transformation for Periodically Driven Systems: Strongly Correlated Systems with Artificial Gauge Fields, Phys. Rev. Lett. **116**, 125301 (2016).

[9] J. H. Mentink, K. Balzer, and M. Eckstein, Ultrafast and reversible control of the exchange interaction in Mott insulators, Nat. Commun. **6**, 6708 (2015).

[10] M. Claassen, H.-C. Jiang, B. Moritz, and T. P. Devereaux, Dynamical time-reversal symmetry breaking and photo-induced chiral spin liquids in frustrated Mott insulators, Nat. Commun. **8**, 1192 (2017).

[11] J. Liu, K. Hejazi, and L. Balents, Floquet Engineering of Multiorbital Mott Insulators: Applications to Orthorhombic Titanates, Phys. Rev. Lett. **121**, 107201 (2018).
[12] K. Hejazi, J. Liu, and L. Balents, Floquet spin and spin-orbital hamiltonians and doublon-holon generations in periodically driven mott insulators, Phys. Rev. B **99**, 205111 (2019).
[13] S. Chaudhary, D. Hsieh, and G. Refael, Orbital floquet engineering of exchange interactions in magnetic materials, Phys. Rev. B **100**, 220403(R) (2019).
[14] N. Arakawa and K. Yonemitsu, Floquet engineering of mott insulators with strong spin-orbit coupling, Phys. Rev. B **103**, L100408 (2021).
[15] A. Ron, S. Chaudhary, G. Zhang, H. Ning, E. Zoghlin, S. D. Wilson, R. D. Averitt, G. Refael, and D. Hsieh, Ultrafast Enhancement of Ferromagnetic Spin Exchange Induced by Ligand-to-Metal Charge Transfer, Phys. Rev. Lett. **125**, 197203 (2020).
[16] S. Chaudhary, A. Ron, D. Hsieh, and G. Refael, Controlling ligand-mediated exchange interactions in periodically driven magnetic materials, arXiv:2009.00813.
[17] G. Jackeli and G. Khaliullin, Mott Insulators in the Strong Spin-Orbit Coupling Limit: From Heisenberg to a Quantum Compass and Kitaev Models, Phys. Rev. Lett. **102**, 017205 (2009).
[18] J. Chaloupka, G. Jackeli, and G. Khaliullin, Zigzag Magnetic Order in the Iridium Oxide Na_2IrO_3, Phys. Rev. Lett. **110**, 097204 (2013).
[19] J. G. Rau, E. K.-H. Lee, and H.-Y. Kee, Generic Spin Model for the Honeycomb Iridates beyond the Kitaev Limit, Phys. Rev. Lett. **112**, 077204 (2014).
[20] S. M. Winter, Y. Li, H. O. Jeschke, and R. Valentí, Challenges in design of Kitaev materials: Magnetic interactions from competing energy scales, Phys. Rev. B **93**, 214431 (2016).
[21] S. M. Winter, A. A. Tsirlin, M. Daghofer, J. van den Brink, Y. Singh, P. Gegenwart, and R. Valentí, Models and materials for generalized Kitaev magnetism, J. Phys.: Condens. Matter **29**, 493002 (2017).
[22] D. Gotfryd, J. Rusnačko, K. Wohlfeld, G. Jackeli, J. C. V. Chaloupka, and A. M. Oleś, Phase diagram and spin correlations of the Kitaev-Heisenberg model: Importance of quantum effects, Phys. Rev. B **95**, 024426 (2017).
[23] J. A. Sears, M. Songvilay, K. W. Plumb, J. P. Clancy, Y. Qiu, Y. Zhao, D. Parshall, and Y.-J. Kim, Magnetic order in α-$RuCl_3$: A honeycomb-lattice quantum magnet with strong spin-orbit coupling, Phys. Rev. B **91**, 144420 (2015).
[24] For simplicity, we impose C_3 symmetry on the hopping matrix elements, however a generalization to account for distortions of the $C2/m$ space group is straightforward.
[25] E.g., a dimensionless field strength of $\bar{A} = 0.25$ at a frequency $\hbar\Omega = 2.5$ eV corresponds to an electric field amplitude of $\mathcal{E} \approx 1.8\times10^7$ V $\cdot$ cm^{-1}.
[26] See Supplemental Material at http://link.aps.org/supplemental/10.1103/PhysRevResearch.4.L032036 for a discussion of Floquet theory, further details of the non-equilibrium model, and photoinduced exchange coefficients for additional pump parameter regimes.
[27] Throughout this study the values of these constants used were adapted from recent *ab initio* and photoemission studies: $U = 3.0$, $J_H = 0.45$, $U' = U - 2J_H$, $\lambda = 0.15$, $\Delta = 5$, $t_1 = 0.03$, $t_2 = 0.03$, $t_3 = -0.06$, $t_4 = -0.02$ and $t_{pd} = -0.9$ [34,36].
[28] Y. Wang, M. Claassen, B. J. Moritz, and T. P. Devereaux, Producing coherent excitations in pumped mott antiferromagnetic insulators, Phys. Rev. B **96**, 235142 (2017).
[29] S. M. Winter, K. Reidl, P. A. Maksimov, A. L. Chernyshev, A. Honecker, and R. Valentí, Breakdown of magnons in a strongly spin-orbital coupled magnet, Nat. Commun. **8**, 1152 (2017).
[30] J. Gordon, A. Catuneanu, E. Sørensen, and H. Y. Kee, Theory of the field-revealed kitaev spin liquid, Nat. Commun. **10**, 2470 (2019).
[31] D. Takikawa and S. Fujimoto, Impact of off-diagonal exchange interactions on the kitaev spin-liquid state of α-$RuCl_3$, Phys. Rev. B **99**, 224409 (2019).
[32] Y. Kawakami, H. Itoh, K. Yonemitsu, and S. Iwai, Strong light-field effects driven by nearly single-cycle 7 fs light-field in correlated organic conductors, J. Phys. B: At. Mol. Opt. Phys. **51**, 174005 (2018).
[33] D. M. Kennes, A. de la Torre, A. Ron, D. Hsieh, and A. J. Millis, Floquet Engineering in Quantum Chains, Phys. Rev. Lett. **120**, 127601 (2018).
[34] H.-S. Kim and H.-Y. Kee, Crystal structure and magnetism in α-$RuCl_3$: An ab initio study, Phys. Rev. B **93**, 155143 (2016).
[35] J. A. Sears, L. E. Chern, S. Kim, P. J. Bereciartua, S. Francoual, Y. B. Kim, and Y. J. Kim, Ferromagnetic Kitaev interaction and the origin of large magnetic anisotropy in α-$RuCl_3$, Nat. Phys. **16**, 837 (2020).
[36] S. Sinn, C. H. Kim, B. H. Kim, K. D. Lee, C. J. Won, J. S. Oh, M. Han, Y. J. Chang, N. Hur, H. Sato, B. Park, C. Kim, H. Kim, and T. W. Noh, Electronic structure of the Kitaev material α-$RuCl_3$ probed by photoemission and inverse photoemission spectroscopies, Sci. Rep. **6**, 39544 (2016).